Biophysical Chemistry 141 (2009) 105–116

Contents lists available at ScienceDirect

Biophysical Chemistry

journal homepage: http://www.elsevier.com/locate/biophyschem

Influence of a lipid bilayer on the conformational behavior of amphotericin B derivatives — A molecular dynamics study

Jacek Czub, Anna Neumann, Edward Borowski, Maciej Baginski *

Department of Pharmaceutical Technology and Biochemistry, Faculty of Chemistry, Gdansk University of Technology, Narutowicza St. 11, 80-952 Gdansk, Poland

ARTICLE INFO

Article history:
Received 4 October 2008
Received in revised form 2 January 2009
Accepted 4 January 2009
Available online 9 January 2009

Keywords:
Amphotericin B
Lipid bilayer
Molecular dynamics
Free energy calculations
Conformational analysis

ABSTRACT

Amphotericin B (AmB) is an effective but very toxic antifungal antibiotic. In our laboratory a series of AmB derivatives of improved selectivity of action was synthesized and tested. To understand molecular basis of this improvement, comparative conformational studies of amphotericin B and its two more selective derivatives were carried out in an aqueous solution and in a lipid membrane. These molecular simulation studies revealed that within a membrane environment the conformational behavior of the derivatives differs significantly from the one observed for the parent molecule. Possible reasons for such a difference are analyzed. Furthermore, we hypothesize that the observed conformational transition within the polar head of AmB derivatives may lead to destabilization of antibiotic-induced transmembrane channels. Consequently, the selective toxicity of the derivatives should increase as ergosterol-rich liquid-ordered domains are more rigid and conformationally ordered than their cholesterol-containing counterparts, and as such may better support less stable channel structure.

1. Introduction

The polyene macrolide antibiotic Amphotericin B (AmB) has been widely used in the clinical treatment of deep-seated fungal infections for more than 45 years. Due to the lack of effective antifungal agents and the ever-increasing population of immunocompromised patients, AmB, despite its severe side effects (e.g., nephrotoxicity), still is recognized as the drug of choice for treating life-threatening mycoses [1,2]. The high therapeutic value of AmB is associated with its advantageous biological properties such as broad antimicrobial spectrum, high fungicidal activity, reluctance to induce a secondary resistance, and activity against multidrug-resistant strains [3,4]. Owing to these properties AmB can be considered as a promising lead compound for the development of novel antifungal drugs [5–7]. Unfortunately, due to the lack of adequate knowledge concerning the AmB's membrane activity mechanism, the development of a new generation AmB based drug has failed. Nevertheless, it seems that rationally designed semisynthetic AmB derivatives with significantly lower toxicity can be obtained [6,8,9] and such compounds definitely could help to improve chemotherapy treatment of systemic fungal infections.

Concerning AmB activity it is well-established that AmB is a membrane-active agent that increases the permeability of the cell membrane of eukaryotic cells to ions and small solutes [10–12]. The phenomenon of AmB-induced membrane alterations leading to cell damage and death is regarded to be a consequence of AmB molecule self-association into the channel-like structures spanning a lipid bilayer [11–15]. It is also commonly accepted that the presence of sterols in the lipid bilayer is essential for the full expression of the channel-forming activity of AmB (at least in the biologically relevant fluid state of the bilayer) [16,17]. The selective toxicity of AmB toward fungal cells, a phenomenon crucial for AmB chemotherapeutic action, is ordinarily attributed to the fact that AmB acts more efficiently in fungal ergosterol-containing membranes than in the mammalian membranes containing cholesterol [10,16,18]. However, the mechanism of selectivity is complex and the role played by sterols in AmB-induced permeabilization has not been unequivocally established. In general, the classical model of AmB membrane action assumes that sterols interact *directly* with antibiotic molecules to form the so-called primary complexes (AmB:sterol) which subsequently associate into a barrel-stave channel [12,14,19]. On the other hand, some authors propose that sterols may act more *indirectly* by modifying the physical properties of the lipid bilayer [12,20,21].

In our laboratory, a series of more selective derivatives of AmB was synthesized and tested in vitro for antifungal activity and toxicity against human cells [8,22–24]. The so-called second generation of derivatives turned out to be the most promising. Chemically, this set of AmB derivatives is characterized by modifications of the two ionizable groups of the parent antibiotic, namely the carboxyl group ($-COO^-$) and the amino group ($-NH^{3+}$). Both of these functional groups are located at the "polar head" part of the antibiotic molecule (Fig. 1). Some of these semisynthetic derivatives, e.g., N-(1-piperidinepropionyl)-amphotericin B methyl ester (PAmE) and N-(N′-3-dimethylaminopropylsuccinimido)-amphotericin B methyl ester (SAmE) (Fig. 1), show a significant increase in selectivity compared to the parent drug

* Corresponding author. Tel.: +48 58 3471596; fax: +48 58 3471144.
E-mail address: maciekb@hypnos.chem.pg.gda.pl (M. Baginski).

0301-4622/$ – see front matter © 2009 Elsevier B.V. All rights reserved.
doi:10.1016/j.bpc.2009.01.001

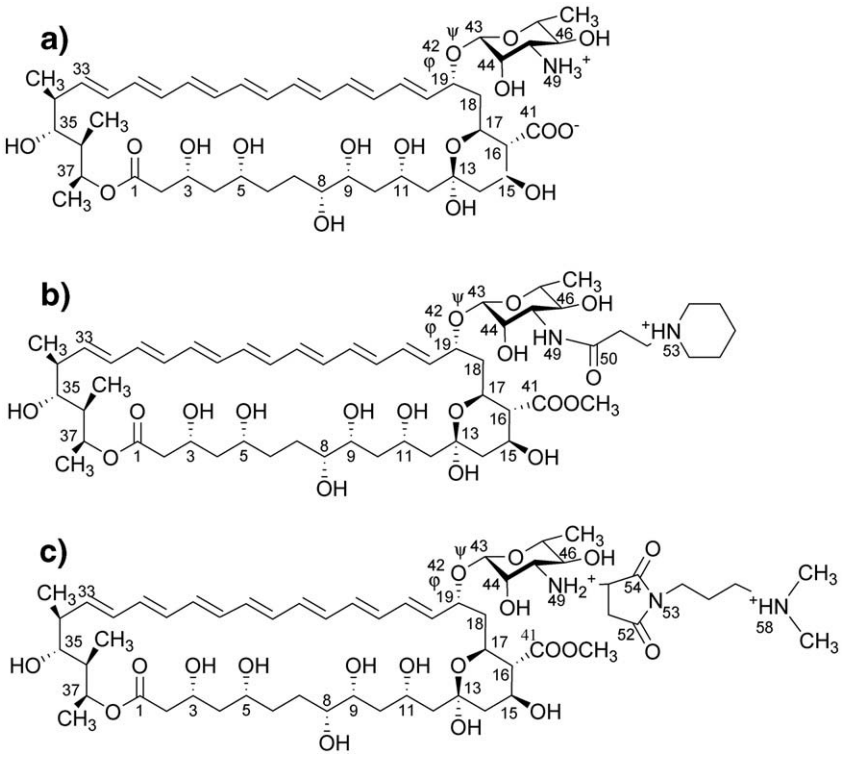

Fig. 1. Chemical structure of AmB (a), PAmE (b) and SAmE (c).

(Table 1) [23,25]. Thus the discussed derivatives can be regarded as a useful testing model to study the molecular basis of the selective toxicity of polyene antibiotics [26].

Some preliminary studies of these compounds have suggested that the covalent modifications of the AmB polar head may induce a change in the orientation of the aminosugar moiety with respect to the relatively rigid macrolide ring (this orientation is defined by the dihedral angles denoted as φ and ψ in Fig. 1) [26,27]. Such conformational transition affects the overall shape of the antibiotic molecules and as a result can change their ability to form various supramolecular complexes, including channel-like structures within a lipid membrane. Thus it appears that this conformational effect should be considered as an important factor determining the biological activity of the antibiotic. The assumption that the mutual orientation of the aminosugar and aglycone may influence the selectivity of AmB (and its derivatives) is also supported by data published by Matsumori et al. who tested another type of AmB derivative [28].

In order to verify the hypothesis that the polar head of AmB derivatives of the second generation undergoes a stable conformational change, the conformational properties of AmB and its two second-generation derivatives (PAmE and SAmE) [22,23] were analyzed in the present work. To do this, the comparative conformational studies on these compounds were carried out in both an aqueous solution and a lipid membrane. It should be stressed that without this comparison it will not be possible to establish whether the conformational behavior observed inside a membrane is just a simple result of the chemical modifications or rather it results from a particular interaction between the modified polar head and a lipid environment.

Conformational analysis of AmB and its derivatives in an aqueous solution was performed by calculating the potentials of mean force (PMFs) for rotations around the C19–O42 and O42–C43 bonds (Fig. 1). In general, PMF (the free energy of a system as a function of a given set of reaction coordinates) determines the dynamics of the system along the chosen degrees of freedom. The remaining degrees of freedom are regarded as a heat bath and thus the chosen sub-system can, for example, be described by a canonical ensemble. Once the PMF is known, the equilibrium probability to find the system in a given state, characterized by certain values of the chosen coordinates, can be easily obtained. Since we were interested in determining the conformational behavior of the antibiotic's polar head, dihedral angles φ (C18–C19–O42–C43) and ψ (C19–O42–C43–C44) were chosen as the reaction coordinates. In previous studies these internal degrees of freedom were shown to be sufficient to characterize the isomeric states of the antibiotic corresponding to various orientations of the aminosugar with respect to the aglycon [29]. To calculate PMFs, first we employed molecular dynamics (MD) simulations together with the two-dimensional umbrella sampling approach (US) [30]. Simulation data were then post-processed using the (periodic and two-dimensional) weighted histogram analysis method (WHAM) [31].

Due to the relatively slow dynamics and the complex structure of a lipid bilayer, it is impossible to obtain (with currently accessible CPU times) a reliable PMF description of the conformational behavior of antibiotic molecules embedded within a membrane. Thus to study the conformational behavior of the antibiotics in the membrane we decided to perform conventional MD simulations, which were expected to show the location of the most populated minima on a conformational free energy landscape. By comparing the MD lipid bilayer results with the PMF aqueous solution profiles, we were also able to

Table 1
Experimental data of antifungal activities and hemolytic properties of studied derivatives collected from our other works

Compound	*C. albicans* IC_{50} [μM]	Hemolysis of erythrocytes EH_{50} [μM]
AmB	0.076[a]	1.8[b]
PAmE	0.140[a]	282.0[a]
SAmE	0.110[c]	153.0[b]

IC_{50} — the concentration of the compound causing 50% of inhibition of fungal growth.
EH_{50} — the concentration of the compound causing 50% hemolysis of erythrocytes.
Superscripts a, b and c denote references 24, 25 and 23 to experimental data, respectively.

identify the main effects of the membrane environment on the conformational properties of the studied antibiotic molecules. To facilitate a comparison of the present results with the previous experimental and computational studies on the AmB and its derivatives DMPC was selected as a model lipid molecule [15,21,28,32–34]. Our previous simulations showed that both cholesterol and ergosterol have only modest effect on the properties of the water/membrane interface [35]. Since the conformational properties of the studied polyenes inside the membrane are determined mainly by the interaction between their polar groups and the interfacial region, we presume that the pure DMPC bilayer rather adequately describes the properties of the membrane environment which are of relevance for our study. The present work is also intended to provide results for comparison with those obtained for the bilayer systems containing physiological amount of sterols. Only such a direct comparison can indicate whether the presence of sterols has an effect on the conformational behavior of AmB and its derivatives. To this end we are currently performing simulations for the systems similar to the ones studied here but containing sterols.

It turned out that within a lipid bilayer the conformation adopted by the two more selective AmB derivatives differ significantly from the one assumed by the parent antibiotic. A possible origin of this difference is also discussed. We also propose a hypothesis that explains why and how the conformational differences observed for the studied derivatives at the molecular level may induce the increase of antibiotic selectivity measured at the macroscopic level [23,25,36].

2. Methods

2.1. PMF calculations

Under the conditions of a constant number of atoms, pressure and temperature (NPT ensemble), the two-dimensional PMF (Gibbs free energy profile), determining the conformational properties of the antibiotic's polar head is defined as:

$$G(\varphi,\psi) = -k_B T \ln \rho(\varphi,\psi) + C, \quad (1)$$

where C is the arbitrary constant and ρ(φ, ψ) is the probability distribution function, which within the classical limit is given as

$$\rho(\varphi,\psi) = \frac{\int dV \int dR \delta(\varphi'[R]-\varphi)\delta(\psi'[R]-\psi)\exp[-(U(R)+PV)/k_B T]}{\int dV \int d\mathrm{R} \exp[-(U(R)+PV)/k_B T]}. \quad (2)$$

The variables φ (C18–C19–O42–C43) and ψ (C19–O42–C43–C44) in the above equations are the dihedral angles defining the mutual orientation of the aminosugar and macrolactone fragments of the antibiotic molecules (Fig. 1); $U(\mathbf{R})$ and V are the potential energy and the volume of the system respectively, and k_B denotes the Boltzmann constant. In principle, it is possible to obtain ρ(φ, ψ), and hence G(φ,ψ), from a long MD simulation. Unfortunately, the convergence of the average (Eq. (2)) is slow due to the presence of energy barriers, and thus currently available computers seem to be insufficient to calculate it within standard MD. To overcome this problem, we employed the commonly used umbrella sampling (US) technique [30]. In this method a series of MD simulations must be performed with the biasing potential centered at given (in our case (φ,ψ)) points to increase the sampling of the different regions of a conformational space.

The NAMD molecular dynamics program was used for all our MD simulations and energy minimizations [37]. The initial geometries of the studied antibiotics were based on a crystal structure [38]. Additional substituents in PAmE and SAmE were built using InsightII software (Accelrys, San Diego, USA). The energy function parameters for the antibiotic molecules were based on the all-atom CHARMM22 force field [39]. The exception were the partial charges, which were obtained by being matched to the molecular electrostatic potential calculated at the semiempirical level of theory [40]. This parameter set was used in our previous studies and proved to give reliable results [21,26,34].

The simulated systems were constructed by inserting a single antibiotic molecule into a rectangular box (38×38×50 Å) of equilibrated TIP3P water molecules. Subsequently, the systems were equilibrated by carrying out short MD simulations; first in NVT (0.5 ns) and then in NPT (2 ns) conditions. Afterwards, the three resulting systems (one for each of the studied antibiotics) were used to generate the initial configurations for the US calculations. For each antibiotic molecule, the conformational space was sampled on an evenly distributed grid of 324 (18×18) US windows for the dihedral angles φ and ψ varying from −180° to +180° with a step of 20°. The initial configurations were prepared by setting the dihedral angles to successive values and next by minimizing the energy of the system using the steepest descent method in two stages. In the first one the whole antibiotic molecule was kept fixed, and in the second, only the φ and ψ angles were frozen. The obtained structures were then subjected to a NPT MD simulation in periodic boundary conditions, with a 2-fs integration step using the leapfrog Verlet algorithm. All bonds involving hydrogen atoms and the bond angle of the water molecules were constrained to fixed values using the SHAKE algorithm [41]. The non-bonded interactions were calculated using a smooth cut-off (15–18 Å). The temperature was kept at 300 K by applying Langevin dynamics to all non-hydrogen atoms with a dumping coefficient of 1.0 ps. The pressure was maintained at 1 bar using a Nose-Hoover Langevin piston barostat with an oscillation period of 100 fs and a damping time of 50 fs [42]. Harmonic biasing potential with a force constant of 0.0152 kcal/(mol*deg^2) was used. In each US window the systems were simulated for 3–4 ns and the last 2 ns were taken to construct the biased distribution function, ρ*(φ,ψ). This distribution was then transformed into ρ(φ,ψ) by employing the two-dimensional weighted histogram analysis method (2D-WHAM) with a bin width of 2.0° and the tolerance for free energy constants at 10^{-4} kcal/mol [31]. The 2D-WHAM method was implemented by us in a way suitable for the periodic nature of the dihedral angles and the biasing potential. Monte Carlo bootstrap method was applied to estimate the statistical uncertainty of the calculated free energy values.

2.2. Molecular dynamics simulations

The simulations of the antibiotic molecules embedded in the DMPC lipid bilayer were performed using the CHARMM27 lipid force field for the phospholipid molecules [43]. In order to prepare the initial structures of the studied systems, we removed four DMPC molecules from the equilibrated and fully-hydrated lipid bilayer. This bilayer, taken from our previous study, contained 100 DMPC in each leaflet solvated by 9531 waters [34]. Two antibiotic molecules were inserted into each membrane layer in such a way as to be isolated/separated from one another. Thus, the constructed systems corresponded to the monomeric state of the antibiotics and the four inserted molecules were only used to improve sampling efficiency. For the same reason, the initial conformations of each derivative were chosen so that two out of four molecules represented the so-called “open state” and the remaining ones represented the so-called “closed state” (see Section 3.1). It is known that the CHARMM force field tends to give underestimated values of the membrane area per lipid molecule when NPT conditions (i.e., the most natural ensemble for lipid bilayers in equilibrium) are applied. Therefore we used a simulation cell with the z dimension (i.e., the normal to the bilayer surface), which could adjust to maintain the normal component of pressure, P_N, equal to 1 bar, and the x and y dimensions, which were fixed to maintain the membrane surface area (NP_NAT ensemble). The mean area per DMPC molecule in a liquid-crystalline bilayer was experimentally determined [44] to be ~61.0 Å^2. The average cross-

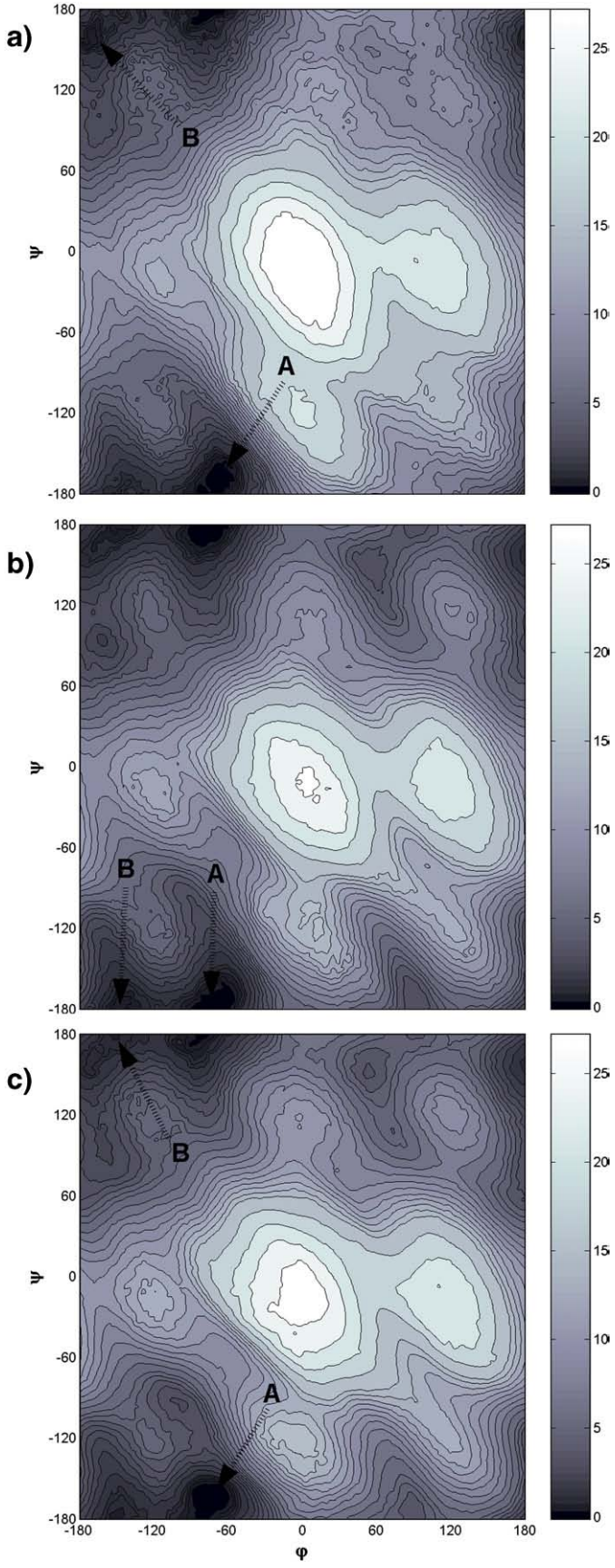

Fig. 2. Potential of mean force for the dihedral angles φ and ψ of AmB (a), PamE (b) and SAmE (c) in kcal/mol. A and B denote the "closed" and "open" conformations, respectively.

sectional area per AmB, as estimated in a monomolecular layer [45], is similar to the DMPC area and equals ~56.0 Å^2. Since both studied derivatives have the cross-section very close to that of AmB [46], we set the area of the *xy* plane, *A*, to be 6084 Å^2 (78×78 Å) in all three of the studied systems. The temperature was kept at 300 K by means of Langevin dynamics. A normal pressure of 1 bar was maintained by employing the Langevin piston method [42]. Electrostatic interactions were estimated using the Particle Mesh Ewald method [47] with a 11.0 Å real-space cut-off and fast Fourier transform grid spacing of approximately 1.0 Å. The Lennard-Jones interactions were calculated using a smooth cut-off approach (9/11 Å). The short-range, non-bonded pair list was updated every 10 MD steps. The equations of motion were integrated using the same scheme as in the case of the water solution simulations. The systems were simulated for 40 ns and the last 30 ns were used for the analysis. From our experience, an equilibration period of 10 ns should be sufficient for all of the analyzed quantities to converge. All molecular images were prepared using the VMD program [48].

To provide additional insight into the conformational behavior of the studied antibiotics, conventional MD simulation were also performed for each of the three molecules present in water environment. It was expected that, by using the same method, a more consistent comparison of the conformations adopted in a lipid bilayer and in an aqueous solution can be obtained. For the purpose of these calculations the system setup described already in Section 2.2 was used. Also a simulation protocol employed was the same except that no restraining potential was applied. All three antibiotics were simulated for 50 ns.

3. Results and discussion

3.1. Conformations in an aqueous solution

The Gibbs free energy profile for rotations around the dihedral angles φ and ψ obtained for the AmB molecule in an aqueous solution is presented in Fig. 2a. It is interesting to note that this profile is quite similar to that observed in a conformational study of AmB in a vacuum [29]. The profiles, both in vacuum and water indicate that at thermal equilibrium possible conformations are confined to a relatively restricted area of (φ,ψ) space. However, the number and depth of minima on (φ,ψ) maps is different in both environments. In water two predominant conformers located quite close to each other were found within this region and named "closed" (φ≈−68.5°, ψ≈−175°) and "open" (φ≈−170°, ψ≈161°) conformations (this terminology will be justified later in the text). Example structures of the open and closed states of the AmB's polar head are shown in Fig. 3. The free energy difference (ΔG) between the two conformations, calculated as the difference in the PMF values at the minima corresponding to both states, reveals that the closed state is 0.340± 0.005 kcal/mol (Fig. 2a) lower in free energy than the open state. This difference means that the probability of finding the AmB molecule in the minimum corresponding to the closed state is 1.79 times higher (at T=300 K) than finding it in the minimum corresponding to the open state. Fig. 2a shows, however, that the free energy basin of the AmB's closed conformation is much broader, as compared to the one corresponding to the open state. Thus a better measure of their relative populations in equilibrium than the simple Boltzmann ratio is required. It can be obtained by integrating the probability density, ρ(φ,ψ), over the two low-energy regions of the conformational space. With this procedure [49] we obtained probability values of 0.67 and 0.29 for the closed and open conformations, respectively. These values, indicating that the closed conformation is 2.3 times more probable than the open one, are consistent with the (φ,ψ)-distribution obtained from the conventional MD simulations of the AmB molecule in water environment (Fig. 4). The relative population of the closed state with respect to the open one, calculated simply as the ratio of the number of MD-generated microstates representing both

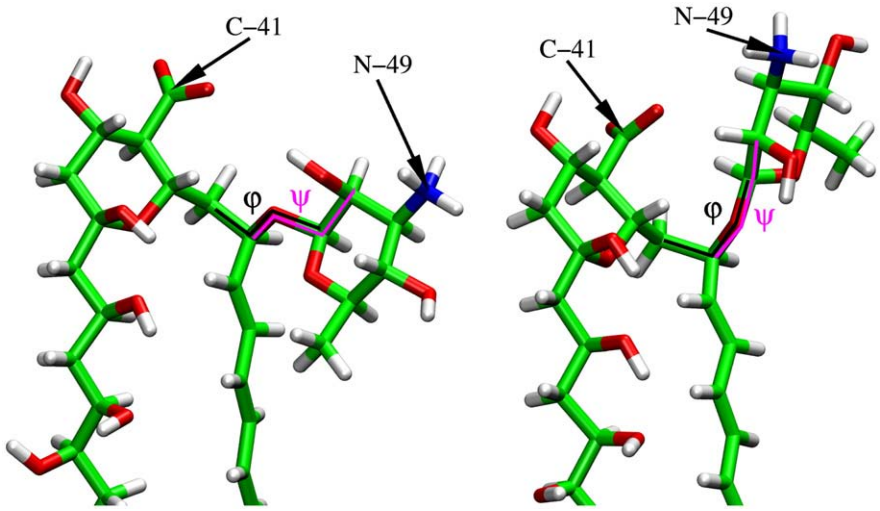

Fig. 3. The open (*left*) and closed (*right*) conformations of AmB's polar head.

conformations, is equal to 2.18. It is worth mentioning that a similar ratio was also observed in the MD simulation where the AmB monomer was present in an aqueous phase near a lipid bilayer [34].

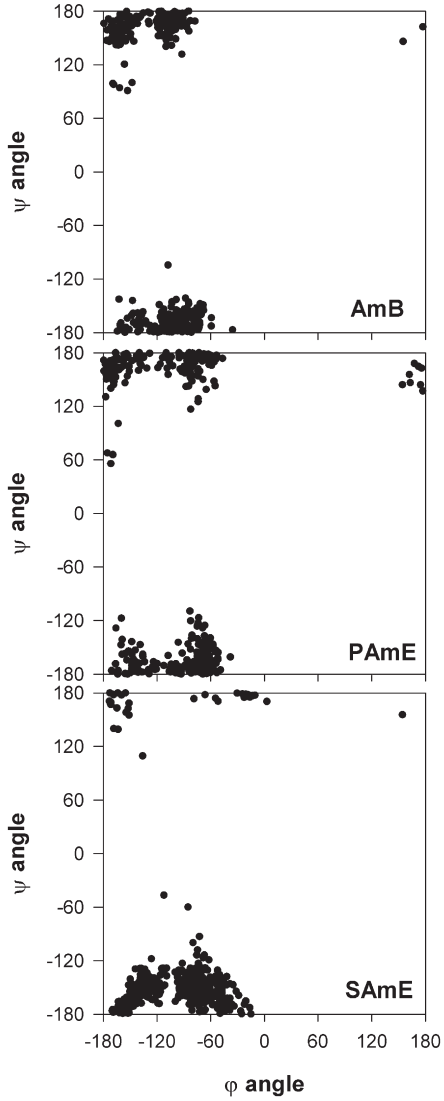

Fig. 4. Distributions of the φ and ψ dihedral angles obtained from the MD simulations of the antibiotic molecules present in an aqueous solution.

The relative population of the two conformational states obtained from the integration of ρ(φ,ψ) over both low-energy regions, namely 2.3, corresponds to the free energy difference of 0.49 kcal/mol. In order to examine the origin of this difference, we decomposed it into individual enthalpic and entropic contributions (Table 2). The enthalpic components were estimated by simply subtracting the average intramolecular interaction energies calculated for the open state from the corresponding energies calculated for the closed state and doing the same with regard to the average solute-solvent interaction energies (the PV term was in each case neglected). The average interaction energies, $\langle E \rangle$, in a given state were obtained by numerically calculating the integral

$$\langle E \rangle = \frac{\int_{state} E(\varphi,\psi)\rho(\varphi,\psi)d\varphi d\psi}{\int_{state} \rho(\varphi,\psi)d\varphi d\psi}, \quad (3)$$

where ρ(φ,ψ) is defined by Eq. (2) and integration is done over the (φ,ψ) region corresponding to this state. E(φ,ψ) function was calculated by averaging individual interaction energy contributions using two-dimensional grid with spacing of 2.0° in each direction. To enhance the convergence of E(φ,ψ), two additional 50-ns-long MD simulations were performed in which φ and ψ angles were restrained to their values in the minima of both conformational states. Because of their importance, the electrostatic contribution to the calculated differences (ΔH_{elec}) are presented separately in Table 2. We also assumed that the solvent-only part of the Hamiltonian is independent of φ and ψ and thus the entropic component (TΔS) could be obtained by simply subtracting the enthalpy change from the overall free-energy difference. The values in Table 2 show that the lower free energy state is stabilized primarily by a favorable electrostatic contribution to the intramolecular enthalpy, arising from the short distance between the oppositely charged groups present in the AmB's polar head ($-COO^-$ and $-NH_3^+$) (Fig. 3). With this intramolecular interaction in mind, this conformer is referred to as the "closed" conformation. On the other

Table 2
Enthalpic ($\Delta H_{B\to A}$) and entropic ($T\Delta S_{B\to A}$) contributions to Gibbs free energy differences $\Delta G_{B\to A}$ between the open (B) and closed (A) states

Molecule	$\Delta G_{B\to A}$ [kcal/mol]	$\Delta H_{B\to A}$ [kcal/mol]				$T\Delta S_{B\to A}$ [kcal/mol]
		intramolecular		molecule-solvent		
		ΔH_{elec}	ΔH_{other}	ΔH_{elec}	ΔH_{vdw}	
AmB	0.49	−29.35	1.68	19.30	−1.89	9.77
PAmE	0.42	−1.18	0.51	−1.53	2.13	−0.49
SAmE	0.48	1.71	2.15	−4.21	1.47	0.64

hand, the second conformational state, in which the two ionized groups are spatially isolated and better hydrated, is referred to as the "open" conformation (Fig. 3). This conformer is stabilized by electrostatic interactions with the solvent. The remaining intramolecular energy terms (their differences are summed, and designated as ΔH_{other} in Table 2) as well as the van der Waals contribution to the solute-solvent interaction energy (ΔH_{vdw}) are very similar for both states. One can also observe that the total enthalpy change, which favors closed conformation, is to a large extent compensated by the entropic term. Since the average solvent accessible surface area (SASA) of AmB is quite similar in both conformational states (i.e., 1212 and 1191 $Å^2$ in the minimum of the closed state and open state, respectively) and consequently, the solvent entropy change is small, we conclude that ΔS arises almost entirely from a difference in the entropy associated with the antibiotic molecule's internal degrees of freedom other than the φ and ψ angles. The lower conformational entropy of the AmB molecule at the minimum of the closed state seems to result from the additional restriction imposed by the COO^-–NH_3^+ intramolecular interaction on the conformational freedom. A further increase of the population difference with respect to the one obtained from Boltzmann ratio should be interpreted as resulting from the higher vibrational entropy caused by the motion along the φ and ψ degrees of freedom.

Fig. 2a also shows that free energy valleys are generally situated along the φ axis. This means that the rotation around the C19–O42 bond is much less restricted than around the O42–C43 bond (ψ axis). Consequently, transitions between the open and the closed state occur along paths roughly parallel to the φ direction.

Fig. 2b and c show the potential of mean force obtained in a water solution for PAmE and SAmE, respectively, as a function of the φ and ψ angles. It is evident that both profiles exhibit similar features as the one calculated for the parent molecule. Again, we can see one region of low free energy with two main minima corresponding to the closed ($\varphi \approx -76.5°$, $\psi \approx -179°$ for PAmE and $\varphi \approx -74.3°$, $\psi \approx -164°$ for SAmE) and the open ($\varphi \approx -158°$, $\psi \approx -179°$ for PAmE and $\varphi \approx -151°$, $\psi \approx 178°$) conformation. In the case of both derivatives the position of the open conformation and, to a lesser extent, that of the closed conformation shifts slightly from what was observed for the parent molecule. However, as in the previous case, the free energy global minimum is located within the closed state. Judging the differences in the PMF values at the minima of the open and closed states ($\Delta G = 0.680 \pm 0.008$ kcal/mol for PAmE and $\Delta G = 0.70 \pm 0.01$ kcal/mol for SAmE), it could be assumed that, compared to AmB, both studied derivatives have a significantly higher tendency to adopt a closed conformation in the aqueous solution. However, integrating the probability density over the relevant regions of the (φ,ψ) space, we found that the probability of PAmE adopting the closed and the open conformation is equal to 0.63 and 0.31, respectively (which gives the relative population of 2.0). For SAmE the corresponding probabilities are 0.66 and 0.29 and the relative population is 2.3. Interestingly, these values, which are close to the ones obtained for the parent molecule, suggest that after the modifications the vibrational entropy associated with φ and ψ starts to favor the open conformation. The above results are also in good agreement with the results obtained using the conventional MD simulations in an aqueous environment (Fig. 4). The relative populations calculated from these simulations are 1.91 and 2.28 for PAmE and SAmE, respectively.

The relative populations of the two conformational states obtained from the integration of ρ(φ,ψ) (Fig. 2b and c) correspond to the free energy difference of 0.42 and 0.48 kcal/mol for PAmE and SAmE, respectively (Table 2). Decomposition of the total free energy differences, performed using the same method as described for AmB above, is presented in Table 2. It reveals that, in the case of AmB derivatives, both enthalpic and entropic contributions are much smaller than for AmB. This, in turn, may be the result of esterification, which removes a charge from the carboxyl group. It seems that rather large uncertainties in the average energy values does not justify further discussion of the small enthalpic and entropic contributions calculated for the derivatives in Table 2.

The PMFs obtained for the two AmB derivatives once again show that rotation around the O42–C43 bond is more restricted than around C19–O42. The transitions between the open and closed states also occur approximately along the direction $\psi = 180°$, which indicates that for the purpose of the future studies on larger sets of derivatives the reaction coordinate may be, in principle, reduced to the φ dihedral angle.

3.2. Influence of membrane environment on antibiotic conformations

We recently published a series of analyses concerning the structural and dynamic properties of AmB and its derivatives (PAmE and SAmE) when embedded within a lipid bilayer [21,26,35,50]. The validation of the lipid bilayer model (DMPC) used in the present work was also made previously [34,51]. Since this DMPC membrane model shows general consistence with experimental results we have decided not to repeat here analyses dedicated to lipid components of the membrane. Instead, this particular paper is focused mainly on the conformational behavior of antibiotic molecules within a phospholipid membrane as it has not been studied in detail before. Various

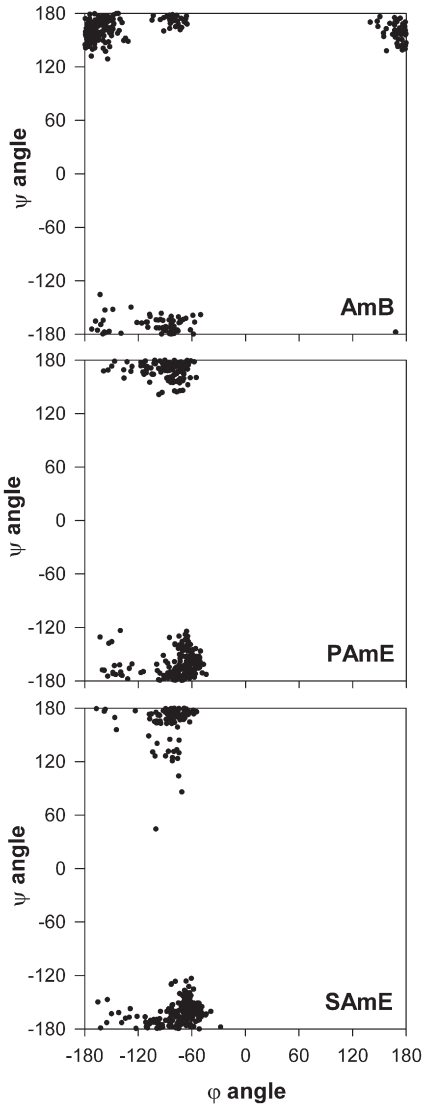

Fig. 5. Distributions of the φ and ψ dihedral angles obtained from the MD simulations of the antibiotic molecules embedded within the DMPC bilayer.

Table 3
The average distance (Å) of the selected atoms form the membrane midplane

Atom type	Simulated system		
DMPC	DMPC/AmB	DMPC/PAmE	DMPC/SAmE
N (choline group)	18.7±0.11	18.5±0.12	18.5±0.14
P (phosphate group)	17.6±0.10	17.5±0.10	17.3±0.12
C (carbonyl *sn*1)	12.7±0.10	12.6±0.10	12.5±0.09
C (carbonyl *sn*2)	13.4±0.10	13.1±0.10	13.0±0.14
C (terminal methyl)	2.9±0.17	3.1±0.17	3.0±0.16
Antibiotic			
N-49	17.0±1.20	15.8±0.70	17.6±0.77
C-41	17.3±1.12	15.5±0.68	16.4±0.88
O-46	15.7±1.28	14.6±0.88	17.1±0.78
O-44	14.5±1.30	13.8±0.70	15.5±0.78
O-15	15.9±1.20	14.9±0.73	16.2±0.87
N-53 (PAmE)	–	18.5±0.72	–
N-58 (SAmE)	–	–	20.2±1.06

associated factors affecting the conformational equilibrium are also discussed in the current work.

The equilibrium distributions of the dihedral angles φ and ψ of AmB and of the two studied derivatives when incorporated into the fluid-phase DMPC bilayer are displayed in Fig. 5 as Ramachandran-like plots. The presented distributions are, to some extent, consistent with the aqueous solution free energy profiles (Fig. 2) and MD-derived (φ,ψ) distributions (Fig. 4) in that only conformers defined above as the open and closed conformations occur within the membrane. However, it is also evident that the membrane environment induces a significant change in the orientation of the aminosugar moiety in relation to the lactone ring when compared to the situation observed in water. In the case of AmB, insertion into the bilayer is associated with a decrease in the closed state population and an increase of the open state population. Thus, whereas the latter state is much less frequent in the aqueous solution, now it becomes the principal conformer of the AmB molecule in the lipid bilayer. An opposite effect, the stabilization of the closed conformation at the expense of the open one, is observed for the two more selective AmB derivatives. Regardless of the initial conditions (for each derivative two molecules were taken from the closed and two from the open conformation), we observed the relaxation to the equilibrium state in which the open conformer appears only incidentally and much less frequently than it follows from the probability value calculated for the systems in the aqueous solution. For each molecule several transitions between the closed and open states were observed (between 4 and 9) which indicates that the relative probabilities seen in Fig. 5 can provide a rather good description of the true equilibrium behavior. One can also notice that the bilayer environment restricts the conformational freedom of the polar heads. This fact could open the possibility of predicting and/or controlling the conformation of the polyene antibiotics within their cellular targets. It is also worth mentioning that the above results are in good agreement with the data of our previous research using GROMACS united atom force field [26].

Determining the molecular basis of the effect of a lipid membrane environment on the conformation of the antibiotic polar head is important as it provides an opportunity to control this conformation by rational chemical modifications of the parent drug. In order to examine this issue, we first calculated the average distance of the selected atoms of the antibiotic and phospholipid molecules from the membrane midplane (Table 3). The obtained data reflect the transverse (along the bilayer normal or the *z* axis) structure of the simulated bilayer systems and show the average location of the antibiotic molecules with respect to the phospholipids constituting the bilayer. The values in Table 3 clearly indicate that the transverse arrangement of the polar head atoms changes significantly as a result of the chemical modifications. The main alteration is the displacement of the esterified carboxyl group (atom C-41) toward the membrane center. As it might have been expected, after esterification, the carboxyl group evades exposure to the water phase. In the PamE case the shift of the carboxyl group (~−2.0 Å) is considerably larger than the one observed for SAmE (~−1.0 Å), showing the general tendency of the former derivative's polar head to penetrate more deeply into the membrane structure (see also the positions of the other functional groups of PAmE in Table 3). On the other hand, we observed that the modified amino groups of the derivatives (atom N-49) also changed their transverse location. However, the magnitude and direction of this displacement differed from the shift of the carboxyl group. Although in the case of PAmE the displacement of the amino group was equal to about −1.1 Å (it shifted toward the membrane center together with the whole polar head), the relative position of this group with respect to the carboxyl group increased from −0.24 to +0.30 Å. Conversely, the modified amino group of SAmE shifted about 0.6 Å in the direction of the water phase and, consequently, its distance to the carboxyl group rose to +0.98 Å. For AmB and SAmE the amino group (atom N-49) resided at approximately the same level of the bilayer structure as the negatively charged DMPC orthophosphoran groups (PO_4^-), suggesting the presence of intermolecular ionic interaction. This positioning effect seemed to weaken when the positive charge of the amino group was removed by the PAmE derivative acylation. As Table 3 shows the additional amino groups of PAmE (piperidine substituent, $-NH(CH_2)_5^+$; atom N-53) and SAmE (dimethylamino group $-NH(CH_3)_2^+$; atom N-58), which are also positively charged, are the subunits most protruded into the water phase. Nevertheless, their distributions along the bilayer normal to some extent overlap with the distributions of the PO_4^- groups. It is particularly noticeable for the more deeply embedded PAmE derivative.

A closer inspection of the trajectories reveals that the studied modifications of the AmB's polar head do not induce a significant change in the average orientation of the whole molecule with respect to the bilayer normal (see, Appendix A). The only thing one can observe is that the deviation from the vertical orientation depends slightly on the average location of the polar head on the *z* axis and increases when the antibiotic molecule penetrates more deeply into the bilayer. With respect to this, the average tilt angle increases as

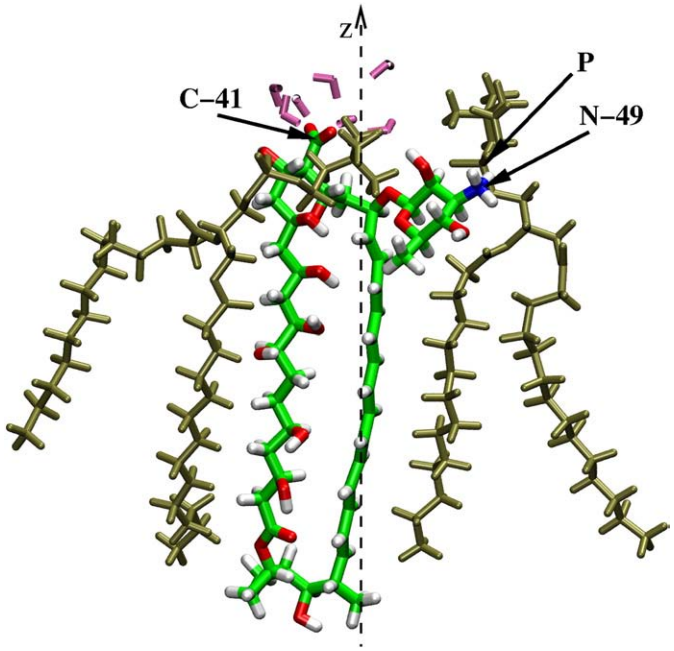

Fig. 6. A typical geometry of AmB observed within the lipid bilayer. The antibiotic molecule adopts the open conformation. Only these water molecules are displayed which were closer than 4 Å from C-41.

follows: SAmE<AmB<PAmE. It seems therefore that a network of interactions in which polar heads participate within the interfacial region of the membrane restricts the wobbling dynamics of the whole antibiotic molecule. This conclusion is consistent with the results of our earlier calculations [26].

As Fig. 1 shows, the amino (atom N-49) and carboxyl groups are attached to the mycosamine and aglycon moieties of the antibiotic molecules, respectively. Since we did not observe significant differences in the overall orientation (tilt angle) of the polyene molecules within the bilayer, the detected changes in the relative position of the atoms C-41 and N-49 have to result directly from the conformational differences between the parent antibiotic and its derivatives (Fig. 5). Representative structures of the AmB and SAmE molecules embedded within the lipid membrane which were taken form the simulations are presented in Figs. 6 and 7, respectively. It can be seen that the open conformation of AmB allows for the interaction of $-NH_3^+$ with the phosphate group of the neighboring DMPC molecule, and, at the same time, for the exposure of $-COO^-$ outside the bilayer. A tendency to stabilize the open conformer in the case of AmB can be also interpreted as the matching of the polar head dipole moment to the lipid headgroup component of the membrane dipole potential. On the other hand, SAmE and PamE, which usually adopt the closed conformation within the membrane, can have their methylated carboxyl groups buried lower in the interfacial region and the modified amino groups located close to the PO_4^- groups of lecithin molecules (Fig. 7). Additionally, in this conformation the positively charged substituents on the N-49 atom of both derivatives are oriented toward the aqueous phase, which would not be the case in the open geometry state.

To obtain a more detailed view of the interactions between the studied polyenes and membrane phospholipids we traced the formation of intermolecular hydrogen bonds between polar groups of these molecules. It should be noticed that, as a result of their chemical structure, DMPC molecules can participate in typical hydrogen bonds only as acceptors, whereas there are many proton donors in the structure of polyene macrolides. Table 4 shows the overall probability of hydrogen bond presence (per one antibiotic molecule) as well as the maximal and average hydrogen bond lifetime calculated for all the proton-donating groups from the antibiotic molecules and all proton-accepting groups of DMPC. The exchange of protons or accepting atoms within a given group was not considered as hydrogen bond breaking. Also the number of protons shared between two interacting groups (i.e., the presence of a single or a multiple hydrogen bond) was not distinguished. Consequently, the probabilities were calculated simply as the (normalized) average number of each hydrogen bond type along the trajectory. We used a geometric criterion for hydrogen bonding which required the D–A distance to be less than 0.35 nm and the D–H–A angle to be larger than 135°, where D, A and H are donor, acceptor and proton, respectively. Table 4 contains data obtained only for these (D, A) pairs for which the probability is higher than 0.1 (the only exception is group NH-49 of PAmE). The hydrogen bonds between the antibiotic amino groups and PO_4^- of phospholipids appear to be the most stable and most likely to occur. Due to the fact that the interacting groups are oppositely charged, the interaction between them is also of an ionic nature, which additionally strengthens the hydrogen-bond connections. For example, it can be noticed that the acylation of the AmB amino group drastically reduces its involvement in hydrogen bonding interactions (see: NH-49 group of PAmE in Table 4). In contrast to acylation, alkylation, which preserves a positive charge at $-NH_3^+$, is even associated with a significant increase of hydrogen bond stability (see: $-NH_2^+$–49 group of SAmE in Table 4). In the case of PAmE, the piperidine ($-NH(CH_2)_5^+$) substituent presumably takes over the role of interacting with the lipid PO_4^- groups. This exchange is the main reason for the aforementioned deeper penetration of the whole PAmE's polar head into the bilayer. Conversely, in the SAmE derivative, for which the amino group NH-49 is involved in the interaction with phospholipids, the positively charged dimethylamino group ($-NH(CH_3)_2^+$) is exposed to the aqueous environment and therefore interacts with PO_4^- rather weakly. It was previously shown that the presence of an ionizable amino group within the polar head of the AmB derivatives is essential for channel-forming activity to occur in chemotherapeutically relevant concentrations [52]. Therefore the current study as well as our earlier simulations [21,26] suggest that the mechanism of polyene-induced permeabilization may require a specific and stable interaction between the antibiotic polar head and the phospholipid headgroups. Such an interaction could, for instance, ensure the proper positioning of a polyene molecule at the water/membrane interface. As it has already been suggested, the observed interaction may be recognized as one of the main factors responsible for the tendency of the mycosamine to stay closer to the water phase

Table 4
The average number (av. num.) and the maximal (Tmax) and average (Tav) lifetime of hydrogen bonds formed between donating groups of the antibiotic molecules and accepting sites of DMPC

Acceptor–donor	Av. num.	Tmax [ps]	Tav [ps]
AmB–DMPC			
NH_3^+–PO_4^-	0.65	5894.9	316.9
OH-46–PO_4^-	0.24	491.2	67.7
OH-15–PO_4^-	0.14	316.4	57.3
OH-46–PO_4^-	0.11	201.5	33.2
PAmE–DMPC			
$NH(CH_2)_5^+$–PO_4	0.49	4895.9	435.8
NH-49–PO_4^-	0.15	416.2	67.5
OH-46–PO_4^-	0.14	1145.8	129.2
SAmE–DMPC			
NH_2^+-49–PO_4^-	0.75	21,649	1069.2
$NH(CH_3)_2^+$–PO_4^-	0.21	1237.2	201.1
OH-15–PO_4^-	0.30	2680.4	145.0
OH-46–PO_4^-	0.19	1030.9	109.2
OH-46–C═O (*sn*-2)	0.21	1885.7	211.9
OH-44–C═O (*sn*-2)	0.19	1237.1	76.1

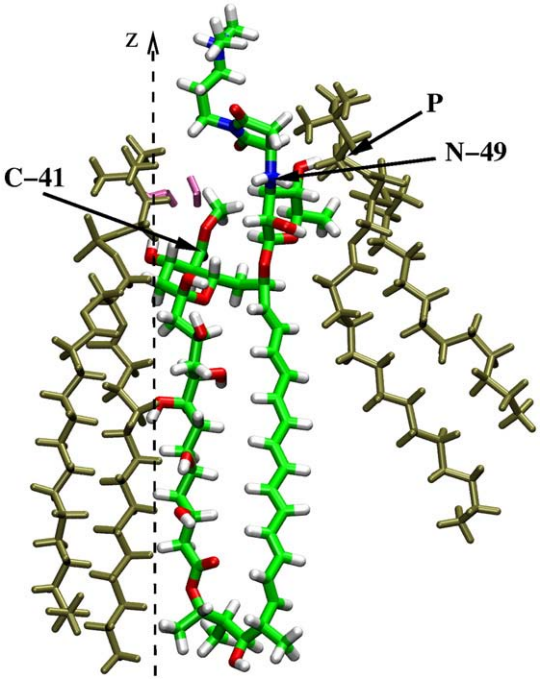

Fig. 7. A typical geometry of SAmE observed within the lipid bilayer. The antibiotic molecule adopts the closed conformation. Only these water molecules are displayed which were closer than 4 Å from C-41.

when compared to the methylated carboxyl group (see also Fig. 7). Hence this effect contributes to the stabilization of the closed conformation of the two studied AmB derivatives. Table 4 also reveals that hydrogen bonds formed by the hydroxyl groups of the antibiotic molecules are in general less stable in comparison with those involving amino groups.

We previously showed that after incorporation into a lipid bilayer, the hydration of polyene molecule polar heads undergoes a substantial change [21,26]. Analysis of differences in the hydration of the important functional groups allows us to examine in what way a bilayer may influence the behavior of antibiotic molecules. For this purpose we calculated the three-dimensional radial distribution functions (RDFs) of water oxygen atoms around the central atoms of selected functional groups of the polar heads (Fig. 8). The RDFs for the antibiotic molecules in an aqueous solution were computed separately for the open and the closed conformations, whereas for molecules embedded in the lipid bilayer the RDFs were averaged over frames in which individual molecules assumed their principal membrane conformations (namely, the closed conformation for PAmE and SAmE and the open conformation for AmB). Fig. 8 shows that RDFs in an aqueous solution only slightly depend on the polar head conformation. For example, as one might expect from the data in Table 2, it can be seen that the considered groups are slightly less hydrated in the closed conformation than in the open one (see, for instance, the RDFs around atom C-41 for all three antibiotics). By integrating the RDFs calculated for AmB in an aqueous solution up to the first minimum and multiplying the result by the overall number density of water molecules, we found that in the open state there are on average 7.3 and 4.7 water molecules in the first solvation layer for $-COO^-$ and $-NH_3^+$ groups, respectively. The corresponding numbers in the closed state are 6.8 and 4.6. The average number of water molecules in the first solvation shell of the PAmE ester ($-COOCH_3$) and acylated amino (atom NH-49) groups (calculated by the integration of the RDF to the same distance as before) in the open state are equal to 3.7 and 1.0, respectively. For SAmE the hydration of the $-COOCH_3$ group is very similar as in the case of PAmE (3.6). One can also notice that the alkylation of $-NH_3^+$ causes significantly less desolvation of this group than the acylation (1.7 water molecules in the first shell around NH_2^+–49 of SAmE in the open state). The transfer of the parent antibiotic from the water phase to the lipid bilayer is associated with a significant decrease in the hydration of the $-NH_3^+$ group (1.6 water molecules in the first shell). Such desolvation was to be expected since it was demonstrated above that $-NH_3^+$ is involved in direct interaction with the PO_4^- groups of phospholipids. On the other hand, it turns out

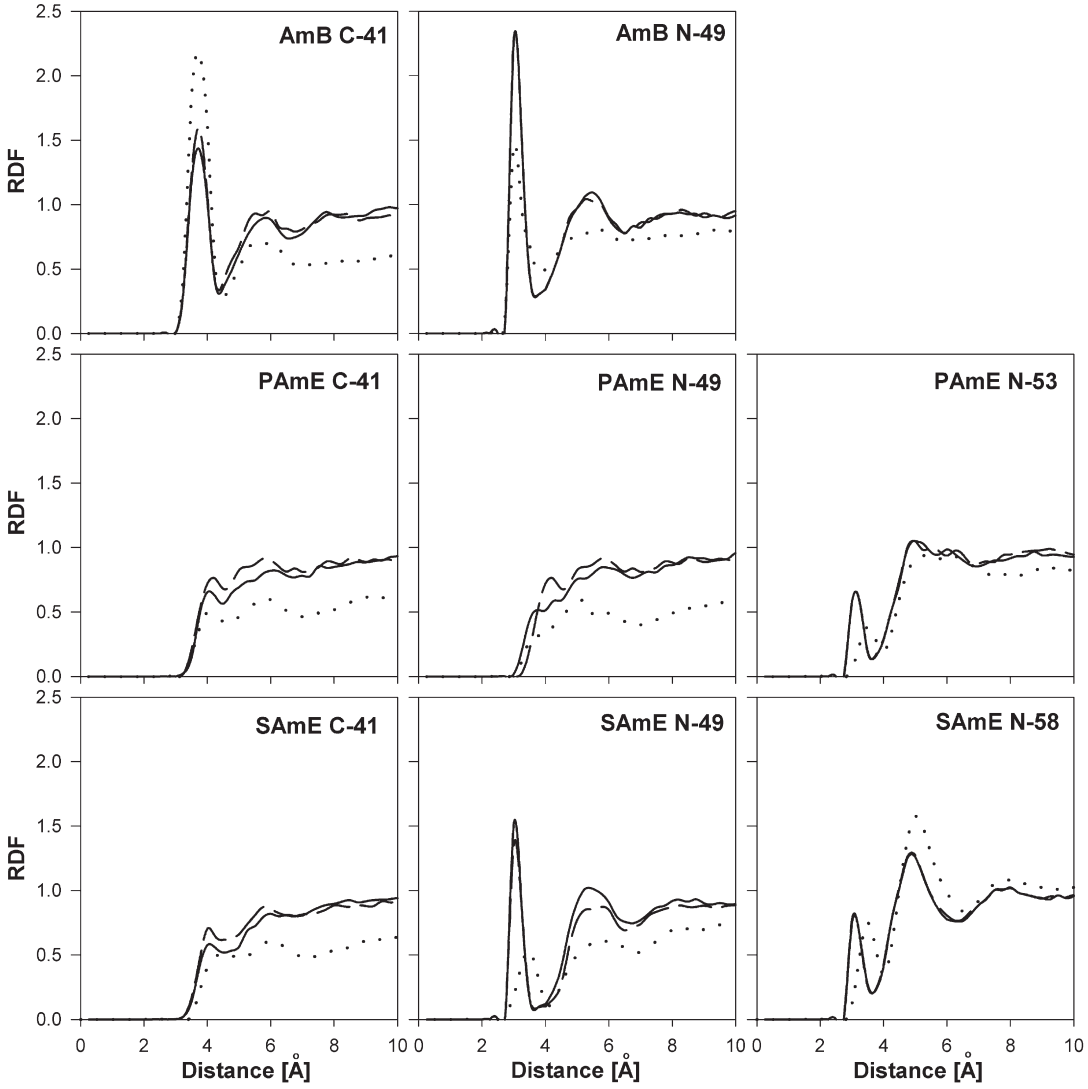

Fig. 8. Three dimensional radial distribution functions for water oxygen atom around the selected atoms of the antibiotic polar head obtained in an aqueous phase for the open conformation (*solid line*) or for the closed conformation (*dashed line*), and in the lipid bilayer (*dotted line*). It should be noted that due to the different overall density of water molecules in both simulation setups, it is not possible to directly compare the heights of corresponding peaks between the aqueous and membrane environments.

that $-COO^-$ remains well-hydrated even after the transfer of AmB to the membrane (5.5 water molecules in the first shell). This high degree of hydration is the reason why, as was shown earlier, $-COO^-$ tends to reside at the membrane surface, thus bringing the whole macrolactone ring close to the water phase (see also Fig. 6). This result is consistent with experimental and simulation data, indicating that a carboxyl group imposes a significant penalty on the free energy of transfer of the solute, to which it is attached, from water into a lipid bilayer ($\Delta G_{COO^-} \approx +5$ kcal/mol, which is the highest value among typical functional groups occurring in organic chemistry) [53,54]. Therefore one can see that the AmB's preference for adopting the open conformation within a lipid bilayer is to a large extent dictated by a tendency of $-COO^-$ to interact with water molecules. Consequently, after the reduction of its polar nature by methylation, the carboxyl group (together with the whole macrolide ring) ends up closer to the membrane center. Thus, in the light of our previous discussion, such modification of the AmB structure favors the closed conformation of the antibiotic's polar head (see also Fig. 7).

3.3. Possible explanations of improved selectivity

The present work has revealed that one of the main effects of the studied chemical modifications of the AmB structure is a significant change in the conformational behavior of antibiotic polar heads. It is worth stressing that, despite the fact that the substituents at N-49 atom in PAmE and SAmE differ chemically, the observed change, that is the population inversion of the open and closed states, is the same. It is also clear that differences in the conformational properties do not appear until the molecules are incorporated into the lipid membrane. This suggests that when designing the modifications of membrane-active compounds (like AmB) one should take into account the heterogeneous and anisotropic structure of the lipid bilayer, and the properties resulting from this complexity, such as the dipole potential and the spatial inhomogeneity of the dielectric constant.

It is widely accepted that AmB-induced permeabilization of lipid bilayers occurs due to the formation of certain associated antibiotic species within the bilayer (e.g., the so-called barrel-stave channel) [11–15]. Since the conformation of the polar head affects the overall shape of a polyene molecule and arrangement of its key functional groups, it may also influence the self-association of antibiotic molecules into conducting aggregates (in terms of both their structure and stability). For example, it has been proposed that the AmB open conformation, which is especially able to participate in the intermolecular interactions (see: Figs. 3 and 6), should be considered as a contributor to the stabilization of a hypothetical model of the barrel-stave AmB channel in its open form [32,33]. This result suggests that the stable transition of the polar head to the closed conformational state, as has been observed for the two studied derivatives of improved selectivity, should lead to the decrease of transmembrane channel stability. There is also some evidence that the full expression of the AmB channel-forming activity occurs within the environment of sterol-enriched, liquid-ordered membrane domains [7,21,55]. These supramolecular structures (e.g., lipid rafts present in the plasma membrane of eukaryotic cells) might be regarded as providing an adequate level of bilayer rigidity for the antibiotic molecules to form of a multimolecular assembly that spans the membrane. Such an assumption is also supported by the observation that, at low (chemotherapeutically relevant) concentrations, AmB is able to permeabilize a sterol-free bilayer in a gel phase, while it is inactive against the same bilayer in an liquid-disordered phase [11,56]. If we take into account that, compared to cholesterol, ergosterol appears to induce a higher degree of internal order in liquid-ordered phases comprising saturated phospholipids [35,57,58], then the conformational transition of the polar head, which decreases the stability of the channel (i.e., loosens its structure), may be recognized as improving the selective toxicity of the antibiotic. Thus one may propose that any modification resulting in a less stable structure of the channel may improve the selectivity of the antibiotic (provided that the modifications do not preclude channel formation). It should be also noted that in the context of the proposed AmB channel model, the nature of the substitutions in PAmE and SAmE (namely the elimination of a carboxyl group charge and the introduction of a bulky substituent to the amino group) can also be seen as lowering the stabilization of the channel and, consequently, as improving the selective toxicity of both compounds. However, earlier experiments in our laboratory have also shown that simply blocking both ionizable groups of the polar head is not sufficient to largely improve the selectivity [52,59].

On the other hand, one can propose another explanation of how the improved selective toxicity of the studied derivatives can arise from their conformational behavior. According to the traditional model of the AmB's mechanism of action, the antibiotic molecules are able to form specific complexes (so-called primary complexes) with sterol molecules. It was also suggested in several previous works that the axial hydroxyl group at atom C-44 (mycosamine moiety) is likely to be involved in stabilizing such complexes by forming a hydrogen bond with the 3β-hydroxyl group of sterols [26,28,33,60]. It can be seen in Figs. 3 and 7 that in the closed conformation OH-44 is positioned with respect to the aglycone part in such a way that may be considered favorable to the formation of a primary complex. In the hypothetical model of such a complex the overall shape of the antibiotic molecule in the closed conformation would allow the sterol molecule to form a hydrogen bond with OH-44 while its flat steroid nucleus simultaneously interacts with the heptaene moiety. With regard to this, the slight selectivity of AmB may appear as a consequence of the antibiotic forming stable and specific primary complexes with ergosterol but not with cholesterol (on account of structural differences between both sterols). In light of the above discussion, the stabilization of the closed conformation in the studied derivatives may be regarded as raising selectivity on account of the fact that it additionally increases the difference in the affinity of the antibiotic towards both sterols. A similar conjecture was also proposed by Matsumori *et al.* to explain the increased selectivity of another type of AmB derivative [28].

4. Conclusions

In the current study we showed that the two model AmB derivatives of the second generation with much improved selectivity exhibit a conformational behavior that differs significantly from the parent molecule. Moreover, this behavioral difference emerges after the molecules are incorporated into a lipid membrane, their cellular target. Two distinct orientations of aminosugar moiety with respect to a macrolactone ring are observed in equilibrium. These are the open conformation, in which the polar head of the antibiotic molecule seems to be more prone to participate in intermolecular interactions, and the closed conformation, in which the possibilities to interact with other molecules are to some extent limited. It was found that in the aqueous solution the parent antibiotic as well as the two studied derivatives were much more inclined to assume the closed conformation than the open one. On the other hand, in the case of AmB a population inversion of both conformations was observed inside the lipid bilayer. The derivatives, on the other hand, preferred to stay in the closed conformation (in fact, the membrane environment even seemed to stabilize this state). We also analyzed possible reasons for this divergence in conformational behavior and concluded that it mainly arises from significant electrostatic differences between AmB and its derivative polar heads. More specifically, we found that the negatively charged (ionized) carboxyl AmB group (attached to the macrolactone ring) tends to stay close to the water phase while the positively charged amino group (attached to the aminosugar moiety) is involved in interactions with the phosphate groups of the DMPC molecules. After esterification, the carboxyl group together with the whole macrolactone is displaced toward the more hydrophobic part of the interface. On the other hand, the modifications

of the amino group did not induce a serious change in the localization of the polar mycosamine residue. The increase in the distance between the position of the modified carboxyl and amino groups on the axis parallel to the membrane normal (projection of the vector connecting these two groups on the z axis — the distance between amino and carboxyl group in the closed conformation is smaller than in the open conformation but projection of this distance on the z axis is reverse) forces a conformational transition toward the closed state.

Concerning our findings, one may try to pose a 'working hypothesis' linking the different conformational behavior of the derivatives with their improved selectivity observed macroscopically. This hypothesis may be regarded as a bit too speculative but, on the other hand, it may facilitate designing new experiments and chemical modifications which can be useful to understand molecular aspects of the selective action of AmB derivatives. According to this hypothesis, the ability of the derivatives to assume the closed conformation is considered as a factor decreasing the stability of the conducting assembly (e.g., the barrel-stave channel). Once the channel complex is less stable, it becomes more sensitive to the micromechanical properties of the surrounding medium (phospholipid membrane). Consequently, the selective toxicity of the derivatives should increase as ergosterol-rich liquid-ordered phases/domains are more rigid and conformationally ordered than their cholesterol-containing counterparts.

Acknowledgment

This research was supported by the Ministry of Science and Higher Education (grant no. N519 035 32/4168) and Gdansk University of Technology (Poland). The authors would like to thank the TASK Computational Center (Gdansk, Poland) for granting CPU time.

Appendix A. Supplementary data

Supplementary data associated with this article can be found, in the online version, at doi:10.1016/j.bpc.2009.01.001.

References

[1] J. Ritter, Amphotericin B and its lipid formulations, Mycoses 45 (2002) 34–38.
[2] M. Kleinberg, What is the current and future status of conventional amphotericin B? Int. J. Antimicrob. Agents 27 (2006) S12–S16.
[3] S. Hartsel, J. Bolard, Amphotericin B: New life for an old drug, Trends Pharmacol. Sci. 17 (1996) 445–449.
[4] D. Ellis, Amphotericin B: spectrum and resistance, J. Antimicrob. Chemother. 49 (2002) 7–10.
[5] J. Szlinder-Richert, J. Mazerski, B. Cybulska, J. Grzybowska, E. Borowski, MFAME, N-methyl-N-D-fructosyl amphotericin B methyl ester, a new amphotericin B derivative of low toxicity: relationship between self-association and effects on red blood cells, Biochim. Biophys. Acta 1528 (2001) 15–24.
[6] E. Borowski, Novel approaches in the rational design of antifungal agents of low toxicity, Farmaco 55 (2000) 206–208.
[7] D.M. Cereghetti, E.M. Carreira, Amphotericin B: 50 years of chemistry and biochemistry, Synthesis (Stuttg.) (2006) 914–942.
[8] J. Grzybowska, P. Sowinski, J. Gumieniak, T. Zieniawa, E. Borowski, N-methyl-N-D-fructopyranosylamphotericin B methyl ester, new amphotericin B derivative of low toxicity, J. Antibiot. 50 (1997) 709–711.
[9] A. Zumbuehl, P. Stano, M. Sohrmann, M. Peter, P. Walde, E.M. Carreira, A novel strategy for bioconjugation: synthesis and preliminary evaluation with amphotericin B, Org. Biomol. Chem. 5 (2007) 1339–1342.
[10] E.F. Gale, Mode of action and resistance mechanisms of polyene macrolides, in: S. Omura (Ed.), Macrolide antibiotics, Academic Press, Inc., Orlando, 1984, pp. 425–455.
[11] J. Bolard, How do the polyene macrolide antibiotics affect the cellular membrane properties? Biochim Biophys Acta 864 (1986) 257–304.
[12] M. Baginski, B. Cybulska, W.I. Gruszecki, in: A. Leitmannova-Liu (Ed.), Interaction of polyene macrolide antibiotics with lipid model membranes, Advances in planar lipid bilayers and liposomes, vol. 3, Elsevier, Amsterdam, 2006, pp. 269–329.
[13] B. De Kruijff, R.A. Demel, Polyene antibiotic-sterol interactions in membranes of acholeplasma laidlawii cells and lecithin liposomes. III. Molecular structure of the polyene antibiotic-cholesterol complexes, Biochim. Biophys. Acta 339 (1974) 57–70.
[14] S.C. Hartsel, C. Hatch, W. Ayenew, How does amphotericin B work?: studies on model membrane systems, J. Liposome. Res. 3 (1993) 377–408.
[15] S. Matsuoka, H. Ikeuchi, N. Matsumori, M. Murata, Dominant formation of a single-length channel by amphotericin B in dimyristoylphosphatidylcholine membrane evidenced by C-13-P-31 rotational echo double resonance, Biochemistry 44 (2005) 704–710.
[16] D. Kerridge, Mode of action of clinically important antifungal drugs, Adven. Microb. Physiol. 27 (1986) 1–72.
[17] M.J. Paquet, I. Fournier, J. Barwicz, P. Tancrede, M. Auger, The effects of amphotericin B on pure and ergosterol- or cholesterol-containing dipalmitoylphosphatidylcholine bilayers as viewed by H-2 NMR, Chem. Phys. Lipids 119 (2002) 1–11.
[18] T. Teerlink, B. De Kruijff, R.A. Demel, The action of pimaricin, etruscomycin and amphotericin B on liposomes with varying sterol content, Biochim. Biophys. Acta 599 (1980) 484–492.
[19] B.E. Cohen, Amphotericin B toxicity and lethality: a tale of two channels, Int. J. Pharm. 162 (1998) 95–106.
[20] I. Fournier, J. Barwicz, P. Tancrede, The structuring effects of amphotericin B on pure and ergosterol- or cholesterol-containing dipalmitoylphosphatidylcholine bilayers: a differential scanning calorimetry study, Biochem. Biophys. Acta 1373 (1998) 76–86.
[21] J. Czub, M. Baginski, Modulation of amphotericin B membrane interaction by cholesterol and ergosterols — a molecular dynamics study, J. Phys. Chem. B 110 (2006) 16743–16753.
[22] A. Czerwinski, W.A. Konig, T. Zieniawa, P. Sowinski, V. Sinnwell, S. Milewski, E. Borowski, New N-alkyl derivatives of amphotericin B. Synthesis and biological properties, J. Antibiot. 44 (1991) 979–984.
[23] J. Bolard, C.H. Garcia, O. Seksek, E. Borowski, J. Grzybowska, Polyene macrolide derivatives, use for vectoring molecules, Polish Patent Application, 1999.
[24] K. Hac-Wydro, P. Dynarowicz-Latka, J. Grzybowska, E. Borowski, N-(1-piperidine-propionyl)amphotericin B methyl ester (PAME) — a new derivative of the antifungal antibiotic amphotericin B: Searching for the mechanism of its reduced toxicity, J. Colloid Interface Sci. 287 (2005) 476–484.
[25] M. Slisz, B. Cybulska, J. Mazerski, J. Grzybowska, E. Borowski, Studies of the effects of antifungal cationic derivatives of amphotericin B on human erythrocytes, J Antibiot. 57 (2004) 669–678.
[26] M. Baginski, A. Tempczyk, E. Borowski, Comparative conformational analysis of cholesterol and ergosterol by molecular mechanics, Eur. Biophys. J. 17 (1989) 159–166.
[27] K. Sternal, Molecular properties and interactions of supramolecular systems formed by amphotericin B derivatives: Analysis by computational chemistry methods. - doctoral thesis (Gdansk University of Technology, Gdansk, 2005).
[28] N. Matsumori, Y. Sawada, M. Murata, Mycosamine orientation of amphotericin B controlling interaction with ergosterol: sterol-dependent activity of conformation-restricted derivatives with an amino-carbonyl bridge, J. Am. Chem. Soc. 127 (2005) 10667–10675.
[29] M. Baginski, P. Gariboldi, P. Bruni, E. Borowski, Conformational analysis of amphotericin B, Biophys. Chem. 65 (1997) 91–100.
[30] G.M. Torrie, J.P. Valleau, Nonphysical sampling distributions in Monte Carlo free-energy estimations: umbrella sampling, J. Comput. Phys. 23 (1977) 187–199.
[31] S. Kumar, D. Bouzida, R.H. Swendsen, P.A. Kollman, J.M. Rosenberg, The weighted histogram analysis method for free-energy calculations on biomolecules. 1. The method, J. Comput. Chem. 13 (1992) 1011–1021.
[32] M. Baginski, H. Resat, J.A. McCammon, Molecular properties of amphotericin B membrane channel: a molecular dynamics simulation, Mol. Pharmacol. 52 (1997) 560–570.
[33] M. Baginski, H. Resat, E. Borowski, Comparative molecular dynamics simulations of amphotericin B-cholesterol/ergosterol membrane channels, Biochim. Biophys. Acta 1567 (2002) 63–78.
[34] K. Sternal, J. Czub, M. Baginski, Molecular aspects of the interaction between amphotericin B and a phospholipid bilayer: molecular dynamics studies, J. Mol. Model. 10 (2004) 223–232.
[35] J. Czub, M. Baginski, Comparative molecular dynamics study of lipid membranes containing cholesterol and ergosterol, Biophys. J. 90 (2006) 2368–2382.
[36] J. Szlinder-Richert, B. Cybulska, J. Grzybowska, J. Bolard, E. Borowski, Interaction of amphotericin B and its low toxic derivative, N-methyl-N-D-fructosyl amphotericin B methyl ester, with fungal, mammalian and bacterial cells measured by the energy transfer method, Farmaco 59 (2004) 289–296.
[37] L. Kale, R. Skeel, M. Bhandarkar, R. Brunner, A. Gursoy, N. Krawetz, J. Phillips, A. Shinozaki, K. Varadarajan, K. Schulten, NAMD2: greater scalability for parallel molecular dynamics, J. Comput. Phys. 151 (1999) 283–312.
[38] W. Mechlinski, C.P. Schaffner, P. Ganis, G. Avitabile, Structure and absolute configuration of the polyene macrolide antibiotic amphotericin B, Tetrahedron Lett. 44 (1970) 3873–3876.
[39] B.R. Brooks, R.E. Bruccoleri, B.D. Olafson, D.J. States, S. Swaminathan, M. Karplus, CHARMM: a program for macromolecular energy, minimization, and dynamics calculations, J. Comput. Chem. 4 (1983) 187–217.
[40] M. Baginski, E. Borowski, Distribution of electrostatic potential around amphotericin B and its membrane targets, Theochem. J. Mol. Struct. 389 (1997) 139–146.
[41] J.P. Ryckaert, G. Cicotti, H.J.C. Berendsen, Numerical integration of the cartesian equations of motion of a system with constraints: molecular dynamics of n-alkanes, J. Comput. Phys. 23 (1977) 327–341.
[42] S.E. Feller, Y. Zhang, R.W. Pastor, B.R. Brooks, Constant pressure molecular dynamics simulation: the Langevin piston method, J. Chem. Phys. 103 (1995) 4613–4621.
[43] S.E. Feller, A.D. Mackerell, An improved empirical potential energy function for molecular simulations of phospholipids, J. Phys. Chem. B 104 (2000) 7510–7515.
[44] N. Kucerka, Y. Liu, N. Chu, H.I. Petrache, S. Tristram-Nagle, J.F. Nagle, Structure of fully hydrated fluid phase DMPC and DLPC lipid bilayers using X-ray scattering from oriented multilamellar arrays and from unilamellar vesicles, Biophys. J. 88 (2005) 2626–2637.

[45] M. Saint-Pierre-Chazalet, C. Thomas, M. Dupeyrat, C.M. Gary-Bobo, Amphotericin B-sterol complex formation and competition with egg phosphatidylcholine: a monolayer study, Biochim. Biophys. Acta 944 (1988) 477–486.
[46] J. Czub, E. Borowski, M. Baginski, Interactions of amphotericin B derivatives with lipid membranes — a molecular dynamics study, Biochim. Biophys. Acta 1768 (2007) 2616–2626.
[47] T. Darden, D. York, L. Pedersen, Particle mesh Ewald: an N*log(N) method for Ewald sums in large systems, J. Chem. Phys. 98 (1993) 10089–10092.
[48] W. Humphrey, A. Dalke, K. Schulten, VMD: Visual molecular dynamics, J. Mol. Graphics 14 (1996) 33–38.
[49] M. Baginski, L. Piela, Theoretical comparison of conformational properties of molecules — conformational probability maps and similarity index, J. Comput. Chem. 14 (1993) 478–483.
[50] M. Baginski, J. Czub, K. Sternal, Interaction of amphotericin B and its selected derivatives with membranes: Molecular modeling studies, Chem. Rec. 6 (2006) 320–332.
[51] I.Z. Zubrzycki, Y. Xu, M. Madrid, P. Tang, Molecular dynamics simulations of a fully hydrated dimyristoylphosphatidylcholine membrane in liquid-crystalline phase, J. Chem. Phys. 112 (2000) 3437–3441.
[52] M. Herve, J.C. Debouzy, E. Borowski, B. Cybulska, C.M. Gary-Bobo, The role of the carboxyl and amino groups of polyene macrolides in their interactions with sterols and their selective toxicity. A 31P-NMR study, Biochim. Biophys. Acta 980 (1989) 261–272.
[53] T.X. Xiang, B.D. Anderson, Substituent contributions to the transport of substituted p-toluic acids across lipid bilayer membranes, J. Pharm. Sci. 83 (1994) 1511–1518.
[54] T.X. Xiang, B.D. Anderson, A computer simulation of functional group contributions to free energy in water and a DPPC lipid bilayer, Biophys. J. 82 (2002) 2052–2066.
[55] A. Coutinho, M. Prieto, Cooperative partition model of nystatin interaction with phospholipid vesicles, Biophys. J. 84 (2003) 3061–3078.
[56] Y. Aracava, S. Schreier, R. Phadke, R. Deslauriers, I.C.P. Smith, Effects of amphotericin B on membrane permeability-kinetics of spin probe reduction, Biophys. Chem. 14 (1981) 325–332.
[57] J.A. Urbina, S. Pekerar, L. Hong-biao, J. Patterson, B. Montez, E. Oldfield, Molecular order and dynamics of phosphatidylcholine bilayer membranes in the presence of cholesterol, ergosterol and lanosterol: a comparative study using 2H-, 13C- and 31P-NMR spectroscopy, Biochim. Biophys. Acta 1238 (1995) 163–176.
[58] Y.W. Hsueh, K. Gilbert, C. Trandum, M. Zuckermann, J. Thewalt, The effect of ergosterol on dipalmitoylphosphatidylcholine bilayers: a deuterium NMR and calorimetric study, Biophys. J. 88 (2005) 1799–1808.
[59] M. Cheron, B. Cybulska, J. Mazerski, J. Grzybowska, A. Czerwinski, E. Borowski, Quantitative structure-activity relationships in amphotericin B derivatives, Biochem. Pharmacol. 37 (1988) 827–836.
[60] M. Baran, J. Mazerski, Molecular modelling of amphotericin B-ergosterol primary complex in water, Biophys. Chem. 95 (2002) 125–133.